Development of mullite-SiC nanocomposites by pyrolysis of filled polymethylsiloxane gels

Gian Domenico Sorarù [a,*], Hans-Joachim Kleebe [b], Riccardo Ceccato [a], Luca Pederiva [a]

[a]*Materials Engineering Department, University of Trento, Via Mesiano 77, I-38050 Trento, Italy*
[b]*Institute for Materials Research (IMA-I), University of Bayreuth, D-95440 Bayreuth, Germany*

Abstract

A modified processing route, which is based on the active filler controlled pyrolysis technique, was followed here to form a homogeneous mullite-SiC nanocomposite. An Al_2O_3-filled polymethylsiloxane was prepared by the in-situ formation of the SiCO network via a sol-gel process. The filled gels obtained in this way show an excellent machinability with conventional surface grinding techniques. Heat treatment up to 1500°C initiated crystallization of mullite, which showed intragranular SiC precipitation. Based on microstructure characterization in conjunction with thermal analysis, a formation mechanism is proposed which includes the glass transition temperature of SiCO as well as its phase sparation into SiO_2 plus nanosized SiC crystallites, giving rise to this new mullite-SiC nanocomposite. © 2000 Elsevier Science Ltd. All rights reserved.

Keywords: AFCOP; Nano-c; Electron microscopy; Mullite; Composites; Polymer precursors; SiC; Sol-gel processes

1. Introduction

Polymer pyrolysis is a relatively new and very promising technique for processing of advanced ceramics in the form of powder particles, thin films and/or protective coatings as well as fibers.[1–4] The major advantages of such polymer-derived materials is their intrinsic homogeneity on the atomic level, the rather low processing temperatures, and the use of established polymer-processing techniques which enable complex shaping. However, the applicability of subsequent polymer pyrolysis to the fabrication of monolithic components is quite difficult, in particular, owing to the high volume shrinkage associated with the polymer-ceramic transition that often leads to the development of intrinsic microcracks.

In general, processing of ceramic monoliths via organometallic compounds involves crosslinking of the starting precursor followed by pyrolysis at elevated temperatures either in inert[1] or reactive atmospheres.[5] The applied heat treatment initiates the organic–inorganic transition and results in the formation of an amorphous covalent ceramic.[6] Annealing at temperatures exceeding 1000°C yields a partially or completely crystallized ceramic material, which commonly reveals both a residual porosity up to 15% and in some cases a high microcrack density. To overcome this latter problem, a modified process, the so-called AFCOP (active filler controlled pyrolysis), has been developed by Greil and co-workers.[7] According to this method, the polymer is partially filled with inert or active powder particles, in order to decrease the shrinkage and to allow the fabrication of bulk, crack free ceramics. When utilizing inert fillers, simply the precursor volume is reduced which lowers the linear shrinkage of the sample. However, employing active fillers, a reaction between the filler particles and the precursor is initiated which typically results in a volume expansion of the reaction product, as compared to the starting compounds. This expansion counteracts the shrinkage during densification and can lead to near-net shaped crack-free components.[8] A number of systems have already been investigated using polysiloxane resins as preceramic polymers filled with different oxide, carbide, or metallic powders. Subsequent pyrolysis of e.g. polysiloxane in controlled atmosphere was reported to lead to various Si oxycar-

* Corresponding author. Tel.: +39-461-882-454; fax: +39-461-881-977.
E-mail address: soraru@ing.unitn.it (G.D. Sorarù).

bide- or oxycarbonitride-based composites such as SiOC–SiC, SiOC–TiC, SiOCN–TiN and SiOCN–BN.[7,8]

The aim of the present work was to exploit this particular processing method for the preparation of homogeneous mullite–SiC nanocomposites. Al_2O_3-filled polysiloxane has been prepared by mixing the alumina powder with methylthriethoxysilane, $MeSi(OR)_3$, and forming in situ the methylsiloxane network around the oxide filler through hydrolysis–condensation reactions (sol-gel process). Heat treatment in inert atmosphere up to 1500°C finally resulted in the formation of a mullite matrix with both alumina and nano-crystalline silicon carbide inclusions. Based on detailed microstructure characterization by scanning and transmission electron microscopy as well as X-ray diffraction, in conjunction with DTA-TG and dilatometric measurements, a reaction mechanism is proposed which rationalizes the observed microstructure evolution.

2. Experimental procedures

2.1. Sample preparation

Methyltriethoxysilane (MTES) (ABCR) and α-Al_2O_3 powder (Alcoa, A16SG) with an average particle size of 0.8 μm were mixed together in a Al/Si molar ratio of 3:1, which was expected to result in the formation of stoichiometric 3:2 mullite ($3Al_2O_3 \cdot 2SiO_2$). The suspension was kept at 70°C under reflux overnight and after cooling to room temperature 3 moles of acidic water (pH = 1, HCl) per mole of Si were added dropwise. The reaction solution was kept under stirring for 10 min, then, to promote the gelation, an ammonia solution (30% wt) was added until a pH value of 9 was reached. The obtained sol was poured into polypropylene test tubes and the gelation occurred within a couple of hours. Samples were left in air for a week and the final drying was performed at 60°C for another week. Obtained samples were monolithic and crack-free (Fig. 1a) and displayed an excellent machinability with conventional surface-machining technology (Fig. 1b). The
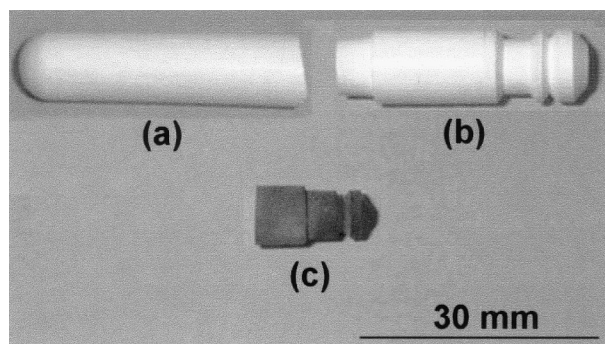
filled gels were converted into the corresponding ceramic samples with the following pyrolysis process: (i) from room temperature to 900°C a tubular silica furnace was used with an heating/cooling rate of 5°C/min and a holding time of 1 h at 900°C, (ii) the ceramic samples obtained after pyrolysis at 900°C were subsequently fired for 1 h at various temperatures, i.e. 1100, 1300, 1400, 1450, and 1500°C in a graphite furnace (Thermal Technology Inc.) with a heating/cooling rate of 10°C/min. All the thermal treatments were performed under flowing argon (100 ml/min) and all the samples obtained were monolithic and crack-free (Fig. 1c).

2.2. Sample characterization techniques

Skeletal densities were measured with a helium pycnometer (Micromeritics, model 1035) while for suitable cylindrical samples the bulk densities were calculated by the ratio mass over volume. Open porosity was determined by the ratio bulk/skeletal density.

Nitrogen adsorption-desorption analyses were performed on an ASAP 2010 Micromeritics instrument. Samples were degassed at 150°C overnight.[9] Isotherm curves were then obtained and specific surface areas were calculated by the BET method in the range of $0.05 \leqslant P/P_0 \leqslant 0.3$. Pore volume and pore size distribution was obtained from the desorption isotherm through the Barret, Joyner and Halenda analysis.[10]

Thermogravimetric (TGA) and differential thermal analyses (DTA) were performed on a Netzsch instrument (model STA 409). Dilatometric curves were monitored by means of a DIL 402 Netzsch dilatometer. TGA/DTA and dilatometric tests were obtained under flowing argon (or in one case in flowing air, see Fig. 6b) with a heating rate of 10°C/min up to a maximum temperature of 1550°C.

X-rays diffraction (XRD) spectra were collected with a Rigaku powder diffractometer in a Bragg–Brentano geometry. CuK_α radiation was used as incident beam

Fig. 1. Typical samples: (a) dried gel; (b) machined gel and (c) mullite–SiC nanocomposite fired in Ar at 1500°C for 1 h.
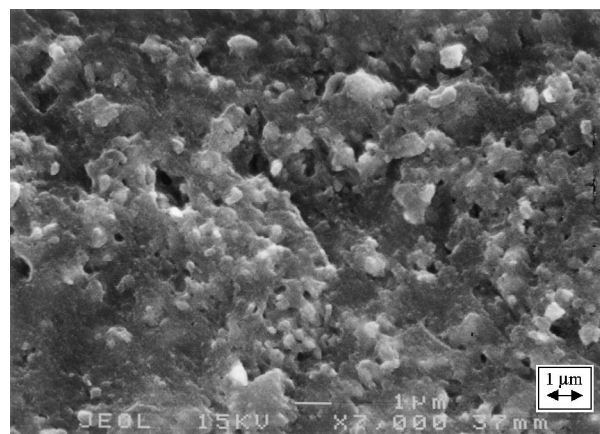

Fig. 2. SEM micrograph of the fracture surface of the Al_2O_3-filled MTES-derived gel.

and a graphite monochromator was inserted into the diffracted beam.

Microstructure characterization was perfomed by both scanning (SEM) and transmission electron microscopy (TEM) employing a Jeol JSM 6300 and a Philips CM20FEG instrument, respectively. While the former microscope was commonly used at 20 keV, the latter instrument was operated at 200 keV, giving a point-to-point resolution of 0.24 nm. Both instruments are equipped with an energy-dispersive X-ray (EDX) Ge-detector (Noran Instruments, Voyager Tracor) allowing for lateral resolved chemical analyses.

3. Experimental results

3.1. Characterization of the gels

Bulk and skeleton densities of the dried gels were 1.49 and 2.44 g/cm^3, respectively. These values give an open porosity of 39%. Nitrogen adsorption–desorption experiments indicate a specific surface area of 110 m^2/g and a total integrated pore volume of 0.220 cm^3/g. SEM observations performed on fracture surfaces of the gel body show a homogeneous dispersion of the alumina powder particles with a grain size smaller than 1 μm (white particles) within the siloxane matrix, as depicted in Fig. 2. No large pores, above ≈1–2 μ, were observed in any of the gel bodies studied. Chemical analysis obtained by EDS (at low magnification) indicated an Al/Si atomic ratio of 2.8±0.1, being close to the nominal value of 3.

3.2. DTA/TG/dilatometric studies

Both DTA and TGA curve recorded on the filled gel during pyrolysis in flowing argon together with its corresponding dimensional changes are shown in Fig. 3. The decomposition of the siloxane matrix results in a major weight loss at around 600°C, due to the evolution of silanes arising from redistribution reactions between Si–O and Si–C bonds.[11,12] The organic–inorganic conversion, with the formation of the SiOC glass, occurs between 700 and 900°C accompanied by the evolution of CH$_4$ and H$_2$.[13] This process is associated with an endothermic effect in the DTA curve (as shown in Fig. 3) centered at ≈800°C and is comparable with data reported in literature.[12,13] The total weight loss between room temperature and 900°C is 11%, which is in good agreement with the value estimated from the weight loss of the pure gel (32%) and the nominal composition of the starting Al$_2$O$_3$-filled gel. From 900°C up to ≈1300°C, the weight of the sample is stable. Above this temperature, however, a slight inflexion of the TGA curve was observed, suggesting the onset for the decomposition of the SiCO glass with the evolution of the volatile SiO and CO species.[14]

In addition to the TGA data the dilatometric curve (also given in Fig. 3) shows a first stage where the sample expands, from room temperature up to ≈300°C. In this temperature interval the siloxane matrix is stable. Above this temperature the decomposition of the siloxane network starts and gives rise to a shrinkage of the material that becomes faster between ≈700 and 850°C. At higher temperatures, the sample's length is almost constant up to about 1300°C where densification starts. This last densification process, which occurs with a very small weight loss as determined by the TG measurements, is most likely due to a viscous sintering of the silicon oxycarbide matrix above its glass transition
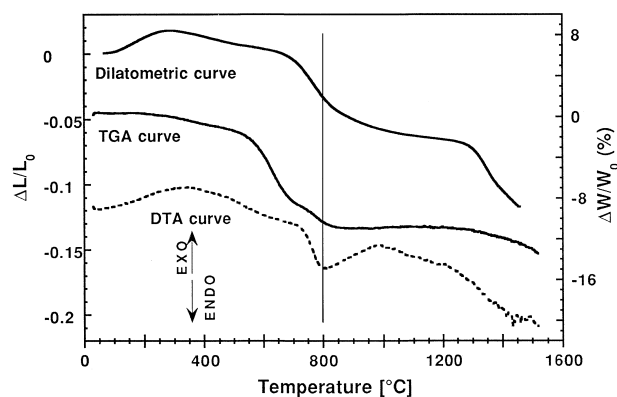

Fig. 3. DTA, TGA and dilatometric curves recorded during pyrolysis in Ar flow on the Al$_2$O$_3$-filled gels.
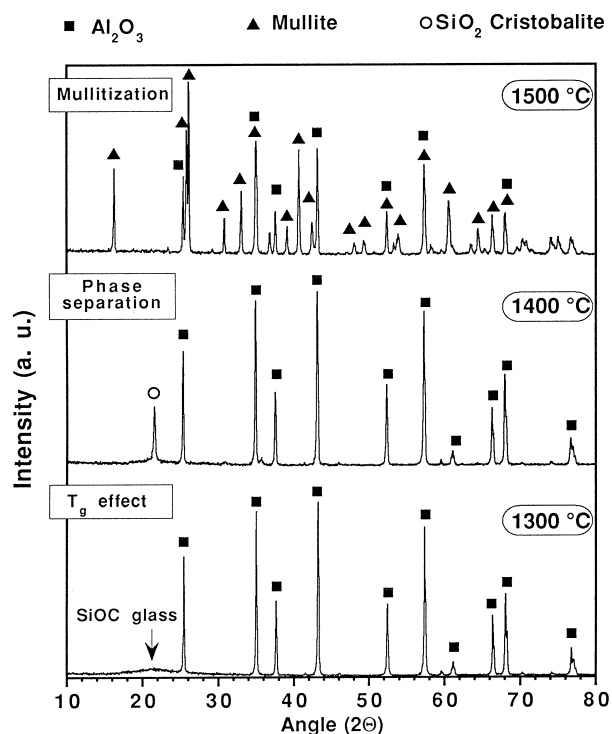

Fig. 4. Evolution of the XRD spectra recorded on the Al$_2$O$_3$-filled gels at various pyrolysis temperatures.
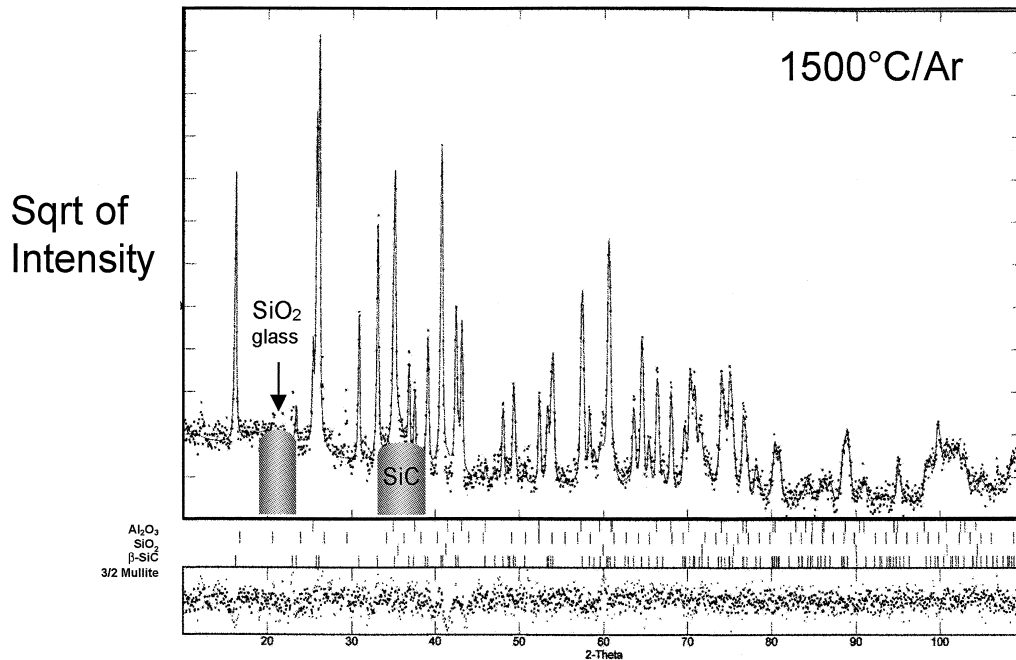
Fig. 5. XRD pattern of the sample pyrolyzed at 1500°C and the corresponding Rietveld fit.
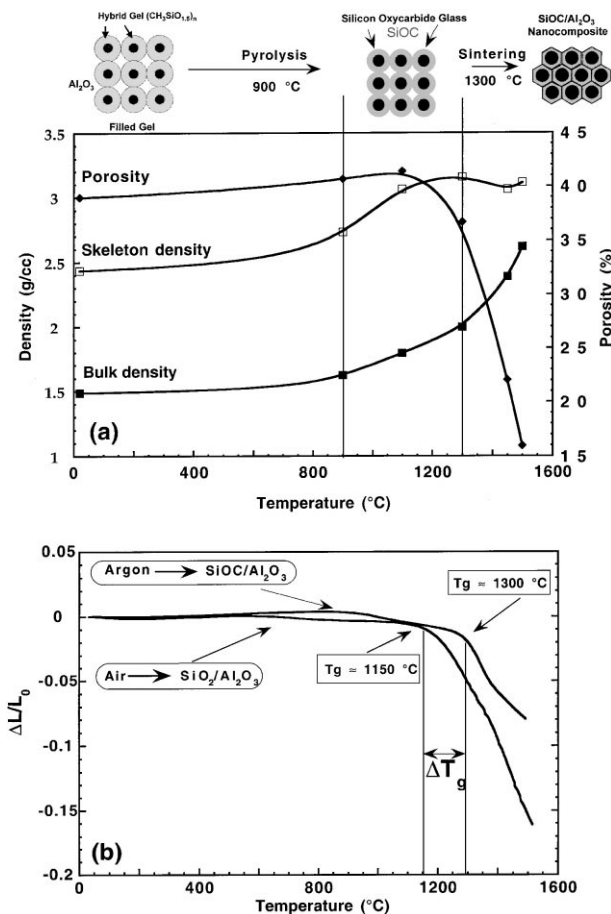

Fig. 6. (a) Plots of bulk density, skeleton density and porosity as a function of pyrolysis temperature in Ar atmosphere; (b) comparison of the dilatometric curves recorded in Ar or air of a sample pre-annealed at 900°C in Ar.

temperature, which is known to be in the range of 1300–1350°C.[15,16]

3.3. Phase development

The phase development, as determined by XRD studies, is depicted in Fig. 4. From room temperature and up to 1300°C, the only crystalline phase that can be detected is α-Al$_2$O$_3$ (JCPDS # 10-173). From 900 to 1300°C, a small glass hump around $2\Theta = 22°$ is due to the presence of the amorphous SiOC phase.[17] At 1400°C, a weak peak at $2\Theta = 22°$ is assigned to the precipitation of cristobalite (JCPDS #39-1425). At 1500°C, the XRD spectrum shows mullite as the major crystalline phase with major reflections at $2\Theta = 15, 30, 32$ and 40° (JCPDS # 15-776), apart from some residual alumina. No cristobalite is present at this temperature. It should be noted that the regular XRD analysis of the 1500°C spectrum did not reveal the presence of SiC. However, by plotting the square root of the intensity vs the diffraction angle 2Θ, as given in Fig. 5, two broad humps centered at ≈35 and $\approx22°$ can be observed, which suggest the formation of rather fine SiC crystallites as well as the presence of residual glass, respectively, which were confirmed by TEM inspection (see Figs. 8 and 9). In addition, this experimental diffraction pattern has been analyzed by the Rietveld method[18] for a quantitative determination of all the phases including mullite, alumina, amorphous silica-based phase, and β-SiC. Details of this XRD data analysis procedure for an ordinary amorphous SiO$_2$/crystalline material (porcelain) and for a similar amorphous SiOC phase are
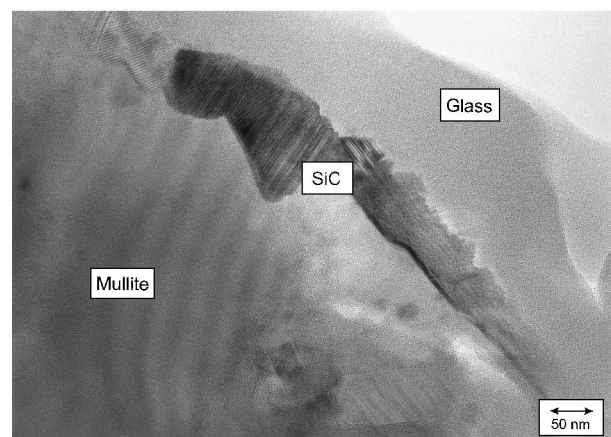
(a)
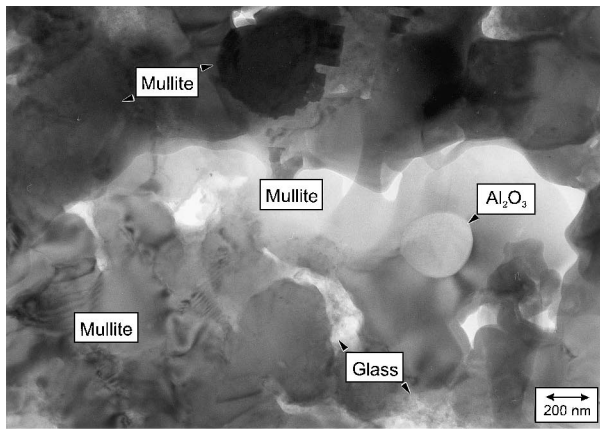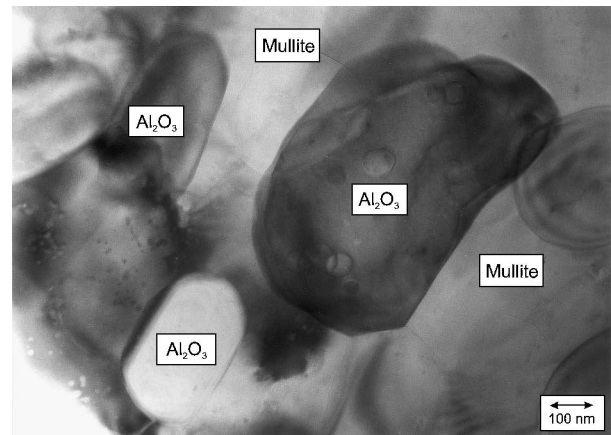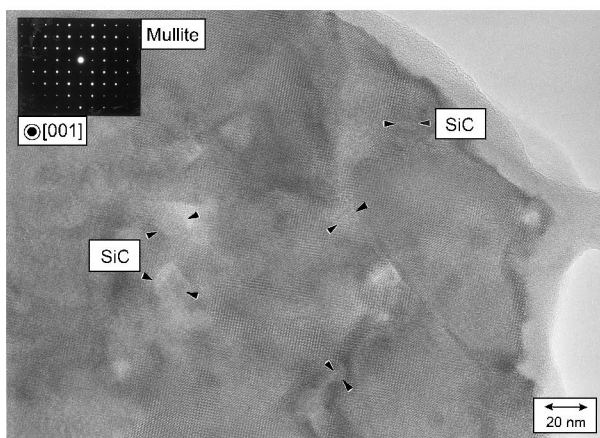
(b)

Fig. 7. (a) Low magnification TEM micrograph of the sample pyrolyzed at 1500°C. Apart from the mullite grains, a spherical alumina particle (200 nm in diameter) and residual glass phase is shown. Note that the glass in fact corresponds to a mixture of SiO_2 and SiC (phase separation); (b) high-magnification TEM micrograph of a mullite matrix grain imaged with the electron beam parallel to the [001] zone axis. As indicated by arrows, small SiC precipitates (5–10 nm in diameter) were typically observed within the mullite particles.

reported elsewhere.[17,19] The results of this calculation are listed in Table 1 and are consistent with the expected formation of a 3:2-mullite–β-SiC composite. The estimated values of the grain size of mullite and β-SiC are ≈60 and 2 nm, respectively, suggesting the formation of a true nanocomposite material. The sample pyrolyzed at 1500°C is mainly formed by mullite (≈66 wt.%), with nanocrystalline silicon carbide (≈7 wt.%), some residual alumina (12 wt.%) and the presence of a glassy phase (15 wt.%) which suggests that the mullitization reaction is in fact not completed yet.

3.4. Microstructure development

Bulk and skeleton densities were measured on samples pyrolyzed in argon at various temperatures, ranging from 900 to 1500°C. The density data together with the estimated open porosity values are listed in Table 2 and

(a)

(b)

Fig. 8. TEM images of the sample pyrolysed at 1500°C revealing (a) residual alumina particles adjacent to mullite matrix grains and (b) a larger SiC precipitate, typically observed at triple grain pockets.

are plotted in Fig. 6a. The skeleton density increases from room temperature up to 1100°C, due to the transformation of the siloxane matrix (density ≈1.1 g/cm^3) into the SiOC glass (density ≈2.3 g/cm^3).[20]

This process results in a parallel increase of the bulk density of the sample without any reduction of the intrinsic porosity, which suggests that the alumina-filled polysiloxane first transforms into the amorphous $SiOC_{matrix}/Al_2O_3$ composite without sintering. On the other hand, above 1100°C, the skeleton density is nearly constant around 3.1 g/cm^3, while the bulk density increases and the porosity decreases, which is a clear indication of a sintering process. In particular, substantial densification occurs above 1300°C, as indicated by the increase of the bulk density from ≈2.00 g/cm^3 at 1300°C up to 2.61 g/cm^3 at 1500°C and by the corresponding decrease of the porosity from 37% at 1300°C down to 16% at 1500°C. Moreover, for the sample pyrolyzed at 1500°C, the BET specific surface area and the total integrated pore volume drop from 110 to 7 m^2/g and from 0.220 cm^3/g to almost zero (0.01 cm^3/g), respectively, as compared to the gel. This densification
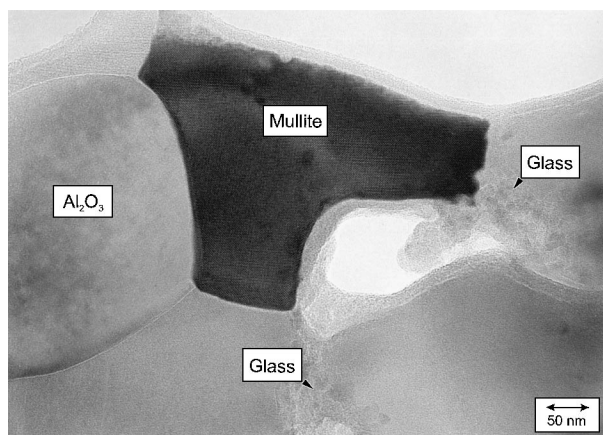
Fig. 9. TEM micrograph of the sample pyrolyzed at 1500°C which shows a mullite grain (in [001] orientation) adjacent to both Al_2O_3 and residual glass phase (being phase-separated). It is concluded that mullite formation occurs via heterogeneous nucleation at the Al_2O_3–SiO/SiC phase boundary.

Table 1
Quantitative analysis and crystallite dimension obtained from the Rietveld analysis of the diffraction pattern of the samples fired at 1500°C

	Mullite	Alumina	SiC	Amorph. SiO_2
Weight %	66	12	7	15
Crystallite size (nm)	58±8	77±9	1.8±0.2	

Table 2
Density and porosity values for the samples pyrolyzed in Ar for 1 h at the indicated temperatures

Temperature (°C)	Bulk density (g/cc)	Skeleton density (g/cc)	Porosity (%)
20	1.49±0.01	2.44±0.01	39
900	1.62±0.01	2.73±0.01	41
1100	1.79±0.01	3.06±0.01	41
1300	2.00±0.01	3.15±0.01	37
1450	2.38±0.01	3.06±0.01	22
1500	2.61±0.01	3.11±0.01	16

process of the amorphous $SiOC/Al_2O_3$ composite in the temperature range between 1300 and 1500°C is certainly due to the viscous sintering of the silicon oxycarbide glass matrix above its T_g which results in the closure of the smaller pores. In Fig. 6b, the comparison of the dilatometric curves recorded in Ar or air of a sample pre-annealed at 900°C in Ar is shown. Heat treatment in air results in both burning of carbon and transformation of the SiOC glass into silica. Consequently, the glass transition temperature is lowered from ≈1300°C for the oxycarbide glass to ≈1150°C, typical for fuse silica. This can be considered as an indirect proof of the presence of a SiOC glass matrix when annealing the filled gels in inert atmosphere.

For the SEM observations, a thin slice was cut from cylindrical pyrolyzed samples and subsequently polished. This sampling procedure allowed to study both the microstructure close to the outer surface and in the core of the cylinder. The central part of the sample is characterized by a rather homogeneous dispersion of residual porosity, with pores generally below ≈3 μm. Even if a quantitative analysis of the SEM images has not been performed, the amount of porosity seems to be consistent with the value of 16% estimated from the bulk and skeleton density measurements already presented. On the other hand, the microstructure at the surface of the rod is different: its porosity level is higher and the pores are larger with dimension up to 10–20 μm. The thickness of this porous layer is ≈0.5 mm for rods being 8 mm in diameter. This porous surface layer is probably due to the incipient decomposition of the silicon oxycarbide phase which leads to the formation of volatile species (SiO and CO) and a porous surface layer.

TEM examination of the central region of a sample pyrolyzed at 1500°C shows a rather complex microstructure (Fig. 7a) where the extensive formation of mullite is evident. The presence of mullite in this material was confirmed by applying both TEM techniques, selected area diffraction (SAD) in addition to energy-dispersive X-ray spectroscopy (EDX). Moreover, the presence of spherical alumina particles in addition to local porosity and residual glass was observed. It should be noted that the residual glass shown here in fact represents a mixture of SiO_2 plus nanosized SiC particles due to the phase separation occuring at temperatures exceeding 1400°C.[21] Moreover, it is important to note that precipitation of nm-sized SiC particles could also be confirmed within the mullite matrix grains by local contrast variations within the high-resolution lattice image of the mullite host crystal (see HRTEM micrograph in Fig. 7b). Typically, the SiC particles are 5–10 nm in size and are seen as intragranular inclusions. In addition to this mullite–SiC nanocomposite microstructure, residual Al_2O_3 particles as well as residual SiCO glass (phase separated) was found (see Fig. 8a and b). This finding is consistent with the reported XRD data and indicates that the formation of mullite was not completed after annealing at 1500°C for 1 h. Apart from the intragranular SiC precipitation, larger SiC particles (up to 100 nm in diameter) were also observed typically at multi-grain junctions, as depicted in Fig. 8(b).

4. Discussion

The new processing technique employed here to form a homogeneous mullite-based nanocomposite is expected to have the following advantages over the conventional AFCOP route: apart from mixing, which can

result in homogeneous green compacts applying both techniques (e.g. molecular nature of liquid silicon alkoxides), (i) the –OH groups at the surface of the oxide particles could react with the Si–OEt and/or the Si–OH surface groups leading to $\equiv$Al–O–Si$\equiv$ bridges thus helping the homogeneous dispersion of Al_2O_3 in the matrix, (ii) the composition of the siloxane network, in terms of Si–R, R = H, Me, Et, ... groups, can be tailored starting from suitable Si–R modified alkoxides, (iii) the introduction in the system of an extra metal such as Zr, Ti, B, etc., could be easily achieved by mixing the Si and Zr, Ti, B, etc., alkoxides, and (iv) the powder-containing sol can be shaped by conventional casting techniques allowing for complex geometries.

SEM study (see Fig. 2) reveals that this new sol-gel process for the synthesis of the Al_2O_3-filled precursor leads to a homogeneous distribution of the alumina powders within the siloxane matrix. Microstructural characterization performed with the nitrogen adsorption-desorption technique suggests that the filled gels are highly porous. This porosity is generated during the drying process of the wet gels and is thought to be related to the constrain induced by the alumina powder on the shrinkage of the gel matrix. Indeed, the linear shrinkage associated to the wet-to-dry gel transformation for an unfilled methyltriethoxysilane-derived sample is 32%, which is much higher as compared to the 20% measured for the filled samples. Moreover, the unfilled gel displays a very low surface area and low pore volume (close to zero), confirming that, when unconstrained, the methylsiloxane gel can shrink during drying without generating any pores.

During pyrolysis in inert atmosphere up to 1100°C, the only phase evolution is associated to the organic-inorganic conversion of the polymethilsiloxane matrix into an amorphous silicon oxycarbide glass. From the microstructural point of view, the level of open porosity does not change (41% at 1100°C), and the increase of the bulk density [from 1.49(1) to 1.79(1) g/cm³; see also Table 2] is simply related to the specific molar volume change of the polymeric matrix upon its conversion into a ceramic material.

Viscous sintering of the glass matrix occurs above 1100°C. The densification rate is the highest above 1300°C, i.e. above the glass transition temperature of the SiCO glass, which is known to be in the range 1300–1350°C.[15,16] Such a viscous sintering process leads to the collapse of most of the finer pores, as it is evident from the nitrogen adsorption-desorption measurement which revealed, for the 1500°C sample, a total pore volume close to zero, as compared to the 0.220 cm³/g of the precursor material.[22]

The observed densification process is similar to the transient viscous sintering (TVS) process developed by Sacks et al.[23] and recently refined by Schneider et al.[24] for the low temperature production of high density mullite ceramics. According to this process, micro-composite alumina powders coated by an amorphous silica layer can be fully densified into an amorphous silica/Al_2O_3 ceramic composite by sintering in the temperature range of 1100–1300°C. Mullite formation can finally take place at temperature in the range 1300–1500°C, depending from the alumina phase employed (α or γ).

As already discussed, in our study, the presence of a silicon oxycarbide glass instead of pure silica accounts for the higher sintering temperature. On the other side, the rather high level of residual porosity ($\approx$16%) observed in our samples can also be related to the larger size of the alumina powder ($\approx$800 nm) compared to those used in the TVS studies (300 nm for the α-Al_2O_3 particles in Ref. 23 and 10 nm for the γ-Al_2O_3 particles in Ref. 24). Indeed, the fine particle size can enhance densification by particle rearrengement. Finally, few large pores which display very low shrinkage rates are probably already present in the Al_2O_3-filled precursor.

One major open question, however, is as to whether the mullite formation proceeds via the classical nucleation and growth process within the glassy phase or if a solid state reaction at the Al_2O_3–SiCO phase boundary is responsible for the mullite nucleation. As shown in Fig. 9, the latter process is thought to be the dominant mechanism, since mullite is formed right at the interface between a residual Al_2O_3 particle adjacent to SiCO glass. It should be also noted that the residual SiCO glass in fact represents a mixture of SiO_2 plus nanosized SiC particles. Indeed, EDX and in particular corresponding EELS analysis of amorphous regions indicates a phase separation of the residual SiCO-glass into SiC nanocrystallites embedded in amorphous silica. A comprehensive study of this phase separation process, which is characteristic for SiOC based glasses at temperatures exceeding 1200°C, is currently ongoing in an European TMR project on SiOC glasses and initial results are presented elsewhere.[17,21]

It is concluded that mullite formation proceeds via a heterogeneous nucleation process at the Al_2O_3–SiO_2/SiC phase boundary and therefore due to this phase separation process, small SiC particles, being 5–10 nm in size, are observed within the mullite matrix grains. Moreover, larger SiC grains are found at grain boundaries and at multi-grain junctions being up to 100 nm in diameter. This reaction mechanism would in turn explain the observed complex microstructure of this mullite–SiC composite.

5. Conclusions

A modified processing route, based on the active filler controlled pyrolysis (AFCOP) process, has been developed for the preparation of ceramic nanocomposites.

The main difference of this processing technique compared with the conventional AFCOP process is the preparation of the starting filled polysiloxane from ceramic powders and a methyl-modified silicon alkoxide, MeSi(OEt)$_3$, through the sol-gel process. The use of a reactive molecular precursor such as MeSi(OEt)$_3$ improves the homogeneous dispersion of the oxide powders into the preceramic matrix, allows a better control of the composition of the preceramic network through the proper choice of the modified silicon alkoxide and, in principle, consents the easy introduction of extra metals such as Zr, Ti, or B via their respective metallic alkoxides. Therefore, it is believed that this modified processing technique can have a great potential to produce a wide range of nano/microcomposites of different composition.

In the present work, this method has been successfully applied for the fabrication of a mullite/SiC nanocomposite in which the SiC nanocrystals are homogeneously dispersed into the mullite matrix grains. The microstructure and phase development during pyrolysis has been investigated by scanning and transmission electron microscopy as well as X-ray diffraction, in conjunction with DTA–TGA and dilatometric measurements. Above 900°C, the A$_2$O$_3$-filled siloxane is tranformed into an amorphous SiOC$_{matrix}$/Al$_2$O$_3$ composite. Around 1300°C this material densifies due to a viscous sintering process of the silicon oxycarbide matrix above its glass transition temperature, which is higher as compared to fused silica. At temperatures exceeding 1350°C, a phase separation of the SiOC glass into SiO$_2$ and nanosized SiC takes place. The silica can then crystallize into cristobalite, as shown by XRD studies. Final mullitization occurs extensively at 1500°C via a reaction of the alumina with the phase separated SiO$_2$ giving the final mullite/SiC nanocomposite. The complexity of the mullite formation mechanism has to be studied in more detail, in order to allow to fully exploit the potential of this process with respect to tailoring of nano/microstructures and respective properties.

Acknowledgements

References

1. Riedel, R., Advances in ceramics from inorganic polymers. In *Materials Science and Technology, A Comprehensive Treatment, Vol. 17B, Processing of Ceramics, Part II*, ed. R. J. Brook. VCH, Wurzburg, 1996, pp. 1–50.

2. Lipowitz, J., Polymer-derived ceramic fibers. *Bull. Am. Ceram. Soc.*, 1991, **70**, 1888–1894.

3. Colombo, P., Paulson, T. E. and Pantano, C. G., Synthesis of silicon carbide thin films with polycarbosilane (PCS). *J. Am. Ceram. Soc.*, 1997, **80**, 2333–2340.

4. Riedel, R., Seher, M. and Becker, G., Sintering of amorphous polymer-derived Si, N and C containing composite powders. *J. Eur. Ceram. Soc.*, 1989, **5**, 113–122.

5. Sorarù, G. D., Sglavo, V. M., Vulcan, F. and Babonneau, F., Fabrication and characterization of β-SiAlON components from polymeric precursors. *Mater. Res. Soc. Symp. Proc.*, 1993, **287**, 245–250.

6. Sorarù, G. D., Babonneau, F. and Mackenzie, J. D., Structural concepts on new amorphous covalent solids. *J. Non-Cryst. Solids*, 1988, **106**, 256–261.

7. Greil, P., Active-filler-controlled pyrolysis of preceramic polymers. *J. Am. Ceram. Soc.*, 1995, **78**, 835–848.

8. Greil, P., Near net shape manufacturing of polymer derived ceramics. *J. Eur. Ceram. Soc.*, 1998, **18**, 1905–1914.

9. Vendange, V. and Colomban, Ph., How to tailor the porous structure of alumina and aluminosilicate gels and glasses. *J. Mater. Res.*, 1996, **11**(2), 518–528.

10. Gregg, S. J. and Sing, K. S. W., *Adsorption, Surface Area and Porosity*. Academic Press, London, 1982.

11. Belot, V., Corriu, R. J. P., Leclercq, D., Mutin, P. H. and Vioux, A., Thermal redistribuition reactions in crosslinked polysiloxanes. *J. Polym. Sci.: Part A: Polym. Chem.*, 1992, **30**, 613.

12. Belot, V., Corriu, R. J. P., Leclercq, D., Mutin, P. H. and Vioux, A., Thermal reactions occurring during pyrolysis of crosslinked polysiloxane gels, precursors to silicon oxycarbide glasses. *J. Non-Cryst. Solids*, 1992, **147 & 148**, 52–55.

13. Campostrini, R., D'Andrea, G., Carturan, G., Ceccato, R. and Sorarù, G. D., Pyrolysis study of methyl-substituted Si–H containing gels as precursors for oxycarbide glasses, by combined thermogravimetric, gas cromatographic and mass spectrometric analysis. *J. Mater. Chem.*, 1996, **6**, 585–594.

14. Bois, L., Maquet, J., Babonneau, F. and Bahloul, D., Structural characterization of sol–gel derived oxycarbide glasses. 2. Study of the thermal stability of the silicon oxycarbide phase. *Chem. Mater.*, 1995, **7**, 975–981.

15. Hammod, M., Breval, E. and Pantano, C. G., Microstructure and viscosity of hot pressed silicon oxycarbide glasses. *Ceram. Eng. Sci. Proc.*, 1993, **14**, 947–954.

16. Rouxel, T., Massouras, G. and Sorarù, G. D., High temperature behavior of an SiOC oxycarbide glass: elasticity and viscosity. *J. Sol-Gel Sci. Technol.*, 1999, **14**, 83–94.

17. Brequel, H., Soraru, G., Babonneau, F., Bahloul-Hourlier, D. and Enzo, S., Structural properties of silicon oxycarbide powders obtained by sol–gel method. *Mater. Sci. Forum*, 1999, **312–314**, 411–416.

18. Young, R. A. *The Rietveld Method*. Oxford University Press, 1993.

19. Lutterotti, L., Ceccato, R., Dal Maschio, R. and Pagani, R., *Materials Science Forum*, 1998, **87**, 278–281.

20. Renlund, G. M., Prochazka, S. and Doremus, R. H., Silicon oxycarbide glasses: part II. Structure and properties. *J. Mater. Res.*, 1991, **6**, 2723–2734.

21. Kleebe, H.-J., Turquat, C. and Sorarù, G. D. Phase separation in a SiCO glass studied by transmission electron microscopy and electron energy-loss spectroscopy. *J. Am. Ceram. Soc.*, submitted for publication.

22. Colomban, Ph. and Vendange, V., Sintering of alumina and mullites prepared by slow hydrolysis of alkoxides: the role of the protonic species and pore topology. *J. Non-Cryst. Solids*, 1992, **147 & 148**, 245–250.

23. Sacks, M. D., Bozkurt, N. and Scheiffele, G. W., Fabrication of mullitea and mullite-matrix composites by transient viscous sintering of composite powders. *J. Am. Ceram. Soc.*, 1991, **74**, 2428–2437.

24. Bartsch, M., Saruhan, B., Schmücker, M. and Schneider, H., Novel low-temperature processing route of dense mullite ceramics by reaction sintering of amorphous SiO_2-coated γ-Al_2O_3 particle nanocomposites. *J. Am. Ceram. Soc.*, 1999, **82**, 1388–1392.